Charged Kaon Interferometric Probes of Space-Time Evolution in Au + Au Collisions at $\sqrt{s_{NN}} = 200$ GeV

S. Afanasiev,[17] C. Aidala,[7] N. N. Ajitanand,[43] Y. Akiba,[37,38] J. Alexander,[43] A. Al-Jamel,[33] K. Aoki,[23,37] L. Aphecetche,[45] R. Armendariz,[33] S. H. Aronson,[3] R. Averbeck,[44] T. C. Awes,[34] B. Azmoun,[3] V. Babintsev,[14] A. Baldisseri,[8] K. N. Barish,[4] P. D. Barnes,[26] B. Bassalleck,[32] S. Bathe,[4] S. Batsouli,[7] V. Baublis,[36] F. Bauer,[4] A. Bazilevsky,[3] S. Belikov,[3,16,*] R. Bennett,[44] Y. Berdnikov,[40] M. T. Bjorndal,[7] J. G. Boissevain,[26] H. Borel,[8] K. Boyle,[44] M. L. Brooks,[26] D. S. Brown,[33] D. Bucher,[29] H. Buesching,[3] V. Bumazhnov,[14] G. Bunce,[3,38] J. M. Burward-Hoy,[26] S. Butsyk,[44] S. Campbell,[44] J.-S. Chai,[18] S. Chernichenko,[14] J. Chiba,[19] C. Y. Chi,[7] M. Chiu,[7] I. J. Choi,[52] T. Chujo,[49] V. Cianciolo,[34] C. R. Cleven,[12] Y. Cobigo,[8] B. A. Cole,[7] M. P. Comets,[35] P. Constantin,[16] M. Csanád,[10] T. Csörgő,[20] T. Dahms,[44] K. Das,[11] G. David,[3] H. Delagrange,[45] A. Denisov,[14] D. d'Enterria,[7] A. Deshpande,[38,44] E. J. Desmond,[3] O. Dietzsch,[41] A. Dion,[44] J. L. Drachenberg,[1] O. Drapier,[24] A. Drees,[44] A. K. Dubey,[51] A. Durum,[14] V. Dzhordzhadze,[46] Y. V. Efremenko,[34] J. Egdemir,[44] A. Enokizono,[13] H. En'yo,[37,38] B. Espagnon,[35] S. Esumi,[48] D. E. Fields,[32,38] F. Fleuret,[24] S. L. Fokin,[22] B. Forestier,[27] Z. Fraenkel,[51,*] J. E. Frantz,[7] A. Franz,[3] A. D. Frawley,[11] Y. Fukao,[23,37] S.-Y. Fung,[4] S. Gadrat,[27] F. Gastineau,[45] M. Germain,[45] A. Glenn,[46] M. Gonin,[24] J. Gosset,[8] Y. Goto,[37,38] R. Granier de Cassagnac,[24] N. Grau,[16] S. V. Greene,[49] M. Grosse Perdekamp,[15,38] T. Gunji,[5] H.-Å. Gustafsson,[28] T. Hachiya,[13,37] A. Hadj Henni,[45] J. S. Haggerty,[3] M. N. Hagiwara,[1] H. Hamagaki,[5] H. Harada,[13] E. P. Hartouni,[25] K. Haruna,[13] M. Harvey,[3] E. Haslum,[28] K. Hasuko,[37] R. Hayano,[5] M. Heffner,[25] T. K. Hemmick,[44] J. M. Heuser,[37] X. He,[12] H. Hiejima,[15] J. C. Hill,[16] R. Hobbs,[32] M. Holmes,[49] W. Holzmann,[43] K. Homma,[13] B. Hong,[21] T. Horaguchi,[37,47] M. G. Hur,[18] T. Ichihara,[37,38] K. Imai,[23,37] M. Inaba,[48] D. Isenhower,[1] L. Isenhower,[1] M. Ishihara,[37] T. Isobe,[5] M. Issah,[43] A. Isupov,[17] B. V. Jacak,[44,†] J. Jia,[7] J. Jin,[7] O. Jinnouchi,[38] B. M. Johnson,[3] K. S. Joo,[30] D. Jouan,[35] F. Kajihara,[5,37] S. Kametani,[5,50] N. Kamihara,[37,47] M. Kaneta,[38] J. H. Kang,[52] T. Kawagishi,[48] A. V. Kazantsev,[22] S. Kelly,[6] A. Khanzadeev,[36] D. J. Kim,[52] E. Kim,[42] Y.-S. Kim,[18] E. Kinney,[6] Á. Kiss,[10] E. Kistenev,[3] A. Kiyomichi,[37] C. Klein-Boesing,[29] L. Kochenda,[36] V. Kochetkov,[14] B. Komkov,[36] M. Konno,[48] D. Kotchetkov,[4] A. Kozlov,[51] P. J. Kroon,[3] G. J. Kunde,[26] N. Kurihara,[5] K. Kurita,[39,37] M. J. Kweon,[21] Y. Kwon,[52] G. S. Kyle,[33] R. Lacey,[43] J. G. Lajoie,[16] A. Lebedev,[16] Y. Le Bornec,[35] S. Leckey,[44] D. M. Lee,[26] M. K. Lee,[52] M. J. Leitch,[26] M. A. L. Leite,[41] H. Lim,[42] A. Litvinenko,[17] M. X. Liu,[26] X. H. Li,[4] C. F. Maguire,[49] Y. I. Makdisi,[3] A. Malakhov,[17] M. D. Malik,[32] V. I. Manko,[22] H. Masui,[48] F. Matathias,[44] M. C. McCain,[15] P. L. McGaughey,[26] Y. Miake,[48] T. E. Miller,[49] A. Milov,[44] S. Mioduszewski,[3] G. C. Mishra,[12] J. T. Mitchell,[3] D. P. Morrison,[3] J. M. Moss,[26] T. V. Moukhanova,[22] D. Mukhopadhyay,[49] J. Murata,[39,37] S. Nagamiya,[19] Y. Nagata,[48] J. L. Nagle,[6] M. Naglis,[51] T. Nakamura,[13] J. Newby,[25] M. Nguyen,[44] B. E. Norman,[26] R. Nouicer,[3] A. S. Nyanin,[22] J. Nystrand,[28] E. O'Brien,[3] C. A. Ogilvie,[16] H. Ohnishi,[37] I. D. Ojha,[49] H. Okada,[23,37] K. Okada,[38] O. O. Omiwade,[1] A. Oskarsson,[28] I. Otterlund,[28] K. Ozawa,[5] D. Pal,[49] A. P. T. Palounek,[26] V. Pantuev,[44] V. Papavassiliou,[33] J. Park,[42] W. J. Park,[21] S. F. Pate,[33] H. Pei,[16] J.-C. Peng,[15] H. Pereira,[8] V. Peresedov,[17] D. Yu. Peressounko,[22] C. Pinkenburg,[3] R. P. Pisani,[3] M. L. Purschke,[3] A. K. Purwar,[44] H. Qu,[12] J. Rak,[16] I. Ravinovich,[51] K. F. Read,[34,46] M. Reuter,[44] K. Reygers,[29] V. Riabov,[36] Y. Riabov,[36] G. Roche,[27] A. Romana,[24,*] M. Rosati,[16] S. S. E. Rosendahl,[28] P. Rosnet,[27] P. Rukoyatkin,[17] V. L. Rykov,[37] S. S. Ryu,[52] B. Sahlmueller,[29] N. Saito,[23,37,38] T. Sakaguchi,[5,50] S. Sakai,[48] V. Samsonov,[36] H. D. Sato,[23,37] S. Sato,[3,19,48] S. Sawada,[19] V. Semenov,[14] R. Seto,[4] D. Sharma,[51] T. K. Shea,[3] I. Shein,[14] T.-A. Shibata,[37,47] K. Shigaki,[13] M. Shimomura,[48] T. Shohjoh,[48] K. Shoji,[23,37] A. Sickles,[44] C. L. Silva,[41] D. Silvermyr,[34] K. S. Sim,[21] C. P. Singh,[2] V. Singh,[2] S. Skutnik,[16] W. C. Smith,[1] A. Soldatov,[14] R. A. Soltz,[25] W. E. Sondheim,[26] S. P. Sorensen,[46] I. V. Sourikova,[3] F. Staley,[8] P. W. Stankus,[34] E. Stenlund,[28] M. Stepanov,[33] A. Ster,[20] S. P. Stoll,[3] T. Sugitate,[13] C. Suire,[35] J. P. Sullivan,[26] J. Sziklai,[20] T. Tabaru,[38] S. Takagi,[48] E. M. Takagui,[41] A. Taketani,[37,38] K. H. Tanaka,[19] Y. Tanaka,[31] K. Tanida,[37,38] M. J. Tannenbaum,[3] A. Taranenko,[43] P. Tarján,[9] T. L. Thomas,[32] M. Togawa,[23,37] J. Tojo,[37] H. Torii,[37] R. S. Towell,[1] V-N. Tram,[24] I. Tserruya,[51] Y. Tsuchimoto,[13,37] S. K. Tuli,[2] H. Tydesjö,[28] N. Tyurin,[14] C. Vale,[16] H. Valle,[49] H. W. van Hecke,[26] J. Velkovska,[49] R. Vértesi,[9] A. A. Vinogradov,[22] E. Vznuzdaev,[36] M. Wagner,[23,37] X. R. Wang,[33] Y. Watanabe,[37,38] J. Wessels,[29] S. N. White,[3] N. Willis,[35] D. Winter,[7] C. L. Woody,[3] M. Wysocki,[6] W. Xie,[4,38] A. Yanovich,[14] S. Yokkaichi,[37,38] G. R. Young,[34] I. Younus,[32] I. E. Yushmanov,[22] W. A. Zajc,[7] O. Zaudtke,[29] C. Zhang,[7] J. Zimányi,[20,*] and L. Zolin[17]

(PHENIX Collaboration)

[1]*Abilene Christian University, Abilene, Texas 79699, USA*
[2]*Department of Physics, Banaras Hindu University, Varanasi 221005, India*

 © 2009 The American Physical Society

[3]Brookhaven National Laboratory, Upton, New York 11973-5000, USA
[4]University of California–Riverside, Riverside, California 92521, USA
[5]Center for Nuclear Study, Graduate School of Science, University of Tokyo, 7-3-1 Hongo, Bunkyo, Tokyo 113-0033, Japan
[6]University of Colorado, Boulder, Colorado 80309, USA
[7]Columbia University, New York, New York 10027, USA, and Nevis Laboratories, Irvington, New York 10533, USA
[8]Dapnia, CEA Saclay, F-91191, Gif-sur-Yvette, France
[9]Debrecen University, H-4010 Debrecen, Egyetem tér 1, Hungary
[10]ELTE, Eötvös Loránd University, H-1117 Budapest, Pázmány P. s. 1/A, Hungary
[11]Florida State University, Tallahassee, Florida 32306, USA
[12]Georgia State University, Atlanta, Georgia 30303, USA
[13]Hiroshima University, Kagamiyama, Higashi-Hiroshima 739-8526, Japan
[14]IHEP Protvino, State Research Center of Russian Federation, Institute for High Energy Physics, Protvino, 142281, Russia
[15]University of Illinois at Urbana-Champaign, Urbana, Illinois 61801, USA
[16]Iowa State University, Ames, Iowa 50011, USA
[17]Joint Institute for Nuclear Research, 141980 Dubna, Moscow Region, Russia
[18]KAERI, Cyclotron Application Laboratory, Seoul, Korea
[19]KEK, High Energy Accelerator Research Organization, Tsukuba, Ibaraki 305-0801, Japan
[20]KFKI Research Institute for Particle and Nuclear Physics of the Hungarian Academy of Sciences (MTA KFKI RMKI), H-1525 Budapest 114, POBox 49, Budapest, Hungary
[21]Korea University, Seoul, 136-701, Korea
[22]Russian Research Center "Kurchatov Institute," Moscow, Russia
[23]Kyoto University, Kyoto 606-8502, Japan
[24]Laboratoire Leprince-Ringuet, Ecole Polytechnique, CNRS-IN2P3, Route de Saclay, F-91128, Palaiseau, France
[25]Lawrence Livermore National Laboratory, Livermore, California 94550, USA
[26]Los Alamos National Laboratory, Los Alamos, New Mexico 87545, USA
[27]LPC, Université Blaise Pascal, CNRS-IN2P3, Clermont-Fd, 63177 Aubiere Cedex, France
[28]Department of Physics, Lund University, Box 118, SE-221 00 Lund, Sweden
[29]Institut für Kernphysik, University of Muenster, D-48149 Muenster, Germany
[30]Myongji University, Yongin, Kyonggido 449-728, Korea
[31]Nagasaki Institute of Applied Science, Nagasaki-shi, Nagasaki 851-0193, Japan
[32]University of New Mexico, Albuquerque, New Mexico 87131, USA
[33]New Mexico State University, Las Cruces, New Mexico 88003, USA
[34]Oak Ridge National Laboratory, Oak Ridge, Tennessee 37831, USA
[35]IPN-Orsay, Universite Paris Sud, CNRS-IN2P3, BP1, F-91406, Orsay, France
[36]PNPI, Petersburg Nuclear Physics Institute, Gatchina, Leningrad region, 188300, Russia
[37]RIKEN Nishina Center for Accelerator-Based Science, Wako, Saitama 351-0198, Japan
[38]RIKEN BNL Research Center, Brookhaven National Laboratory, Upton, New York 11973-5000, USA
[39]Physics Department, Rikkyo University, 3-34-1 Nishi-Ikebukuro, Toshima, Tokyo 171-8501, Japan
[40]Saint Petersburg State Polytechnic University, St. Petersburg, Russia
[41]Universidade de São Paulo, Instituto de Física, Caixa Postal 66318, São Paulo CEP05315-970, Brazil
[42]System Electronics Laboratory, Seoul National University, Seoul, Korea
[43]Chemistry Department, Stony Brook University, Stony Brook, SUNY, New York 11794-3400, USA
[44]Department of Physics and Astronomy, Stony Brook University, SUNY, Stony Brook, New York 11794, USA
[45]SUBATECH (Ecole des Mines de Nantes, CNRS-IN2P3, Université de Nantes) BP 20722 - 44307, Nantes, France
[46]University of Tennessee, Knoxville, Tennessee 37996, USA
[47]Department of Physics, Tokyo Institute of Technology, Oh-okayama, Meguro, Tokyo 152-8551, Japan
[48]Institute of Physics, University of Tsukuba, Tsukuba, Ibaraki 305, Japan
[49]Vanderbilt University, Nashville, Tennessee 37235, USA
[50]Waseda University, Advanced Research Institute for Science and Engineering, 17 Kikui-cho, Shinjuku-ku, Tokyo 162-0044, Japan
[51]Weizmann Institute, Rehovot 76100, Israel
[52]Yonsei University, IPAP, Seoul 120-749, Korea
(Received 28 March 2009; published 30 September 2009)

Bose-Einstein correlations of charged kaons are used to probe Au + Au collisions at $\sqrt{s_{\rm NN}} = 200$ GeV and are compared to charged pion probes, which have a larger hadronic scattering cross section. Three-dimensional Gaussian source radii are extracted, along with a one-dimensional kaon emission source function. The centrality dependences of the three Gaussian radii are well described by a single linear function of $N_{\rm part}^{1/3}$ with a zero intercept. Imaging analysis shows a deviation from a Gaussian tail at $r \gtrsim 10$ fm, although the bulk emission at lower radius is well described by a Gaussian. The presence of a non-Gaussian tail in the kaon source reaffirms that the particle emission region in a heavy-ion collision is

extended, and that similar measurements with pions are not solely due to the decay of long-lived resonances.

DOI: 10.1103/PhysRevLett.103.142301 PACS numbers: 25.75.Dw, 25.75.Gz

Experiments at the Relativistic Heavy-Ion Collider (RHIC) at Brookhaven National Laboratory have revealed that collisions of Au ions at $\sqrt{s_{\rm NN}} = 200$ GeV produce a new form of matter which is opaque to jets and exhibits anisotropic flow consistent with perfect fluid hydrodynamics [1,2]. Studies of the space-time evolution of the collisions are needed to elucidate the properties of the hot, dense, and strongly interacting matter, probe the time scale and degree of thermalization, and investigate the order of the deconfinement phase transition.

Two-particle interferometry, also known as HBT after the radio astronomers Hanbury Brown and Twiss [3], is a powerful tool for measuring the space-time extent of particle-emitting sources. In elementary particle and nuclear physics, enhanced production of like-sign pions with small relative momenta was discovered experimentally and explained by the Bose-Einstein symmetrization of identical bosons [4]. Correlations are produced by the combination of quantum mechanical interference of identical particles and strong and/or electromagnetic final state interactions such as Coulomb repulsion for same-sign charged pairs. HBT radii refer to Gaussian measures of source sizes on the femtometer scale.

Although the traditional HBT analyses are constrained by the assumption of a Gaussian distribution of particle emission, recent detailed measurements of pion emission sources using an imaging technique show a non-Gaussian structure for the two-particle source region above ~20 fm [5], suggesting the possibility that decays of long-lived resonances or a temporal component of the source contribute to the non-Gaussian tail [6]. While charged pions are strongly affected by rescattering among hadrons and decays of hadronic resonances, charged kaons have smaller rescattering cross sections than charged pions ($\sigma_{K-N} < \sigma_{\pi-N}$) and are less affected by resonance decays. Most hydrodynamic models predicted prolonged particle emission durations and correspondingly enlarged HBT radii as a signal of an equilibrium first order phase transition from QGP to hadrons at RHIC energies. However, all of the pion HBT radii measured at RHIC show only slight increases from lower-energy measurements that are far below the theoretical predictions [7]. Because kaons are much less affected by resonance decays than pions, the kaon measurements described herein add an important new constraint to address this "HBT puzzle" [8,9].

An angle-averaged one-dimensional Gaussian measurement of correlations of neutral kaons by STAR [10] suggests that the transverse-mass-dependent HBT radii for neutral kaons and charged pions fall on the same universal curve. In this Letter, 3D Gaussian HBT correlations of like-sign kaons are presented in three transverse momentum bins for $0.3 < p_T < 1.5$ GeV/c and three collision centrality bins. The resulting HBT radius parameters for kaons are compared to those of like-sign pion pairs [11]. In addition we present 1D emission source functions for charged kaons in relativistic heavy-ion collisions.

This analysis of 2004 data from the PHENIX detector [12] uses $\sim 6 \times 10^8$ minimum bias events, which are triggered by the coincidence of the beam-beam counters (BBC) and zero-degree calorimeters (ZDC) with collision vertex $|z| < 30$ cm. A Monte Carlo Glauber model [13] is used to match the observed BBC and ZDC distributions and to bin the data according to the number of nucleons participating in the collisions, $N_{\rm part}$.

Charged kaons are tracked and identified using the drift chamber (DC), pad chambers (PC1,PC3), and PbSc electromagnetic calorimeters (EMCal) to cover pseudorapidity $|\eta| < 0.35$ and azimuthal angle $\Delta\phi = \pi/2$ ($\Delta\phi = \pi/4$) in one (and the other) central arm. A track model provides a three-dimensional trajectory and momentum vector for charged particles based on DC and PC1 information with a momentum resolution of $\delta p/p \simeq 0.7\% \oplus 1.0\% \times p(\mathrm{GeV}/c)$. Backgrounds are reduced by requiring 2σ position match between track projections and EMCal hits, and 3σ match for PC3. Kaons are separated from pions up to $p_T \sim 0.9$ GeV/c using timing information from BBC and EMCal. Particles at higher p_T that fall within 2σ of the ideal mass squared for kaons but $\geq 3\sigma$ away from the peak for pions or (anti-)protons are identified as kaons. The contamination level is ~4% from pions, and ~1% from protons at $p_T \sim 1.5$ GeV/c.

The correlation function is experimentally measured as $C_2(\mathbf{q}) = A(\mathbf{q})/B(\mathbf{q})$ where $A(\mathbf{q})$ is the relative momentum ($\mathbf{q}$) distribution of actual pairs obtained by all possible combinations of pairs within the same events and $B(\mathbf{q})$ is the background pair distribution from mixed events. Two-track detection inefficiencies for charged kaons that traverse the DC and EMCal in close proximity have been carefully studied with Monte Carlo detector simulation and the actual pair distribution is corrected by the MC efficiency factors. After pair selection cuts to remove track splitting and merging (see [11] for details), $\sim 1.5 \times 10^7$ positive kaon pairs, and $\sim 1.4 \times 10^7$ negative kaon pairs remain.

To measure multidimension source sizes, $\mathbf{q}$ is decomposed into standard "side-out-long" axes [14]: for which $q_{\rm long}$ is parallel to the beam axis, $q_{\rm out}$ is parallel to the transverse momentum of the pair [$k_T = (p_{1T} + p_{2T})/2$],

and $q_{\rm side}$ is orthogonal to both $q_{\rm long}$ and $q_{\rm out}$. This analysis is performed in the longitudinally comoving system defined as $p_{1Z} = -p_{2Z}$. For the treatment of charged kaons emitted away from the central region (core), we adopt an effective core-halo Coulomb correction, proposed by Bowler and Sinyukov [15], in which the 3D Gaussian fit function is given by

$$C_2 = C_2^{\rm core} + C_2^{\rm halo} = [\lambda(1+G)]F_C + [1-\lambda], \qquad (1)$$

where the Coulomb correlation function F_C is iteratively evaluated from the Coulomb wave function of kaon pairs assuming a spherical Gaussian source. The Gaussian correlation function in the side-out-long decomposition is determined by

$$G = \exp(-R_{\rm side}^2 q_{\rm side}^2 - R_{\rm out}^2 q_{\rm out}^2 - R_{\rm long}^2 q_{\rm long}^2). \qquad (2)$$

The systematic error estimate incorporates a contribution from the Coulomb interaction of the source halo using a prescription developed by Maj and Mrowczynski [16]. The fitted $R_{\rm side}$ and $R_{\rm long}$ are Gaussian measures of the spatial lengths of homogeneity, where particles of similar momenta are emitted [17], in the transverse and longitudinal directions at freeze-out. $R_{\rm out}$ contains a contribution from the duration of the particle emission in addition to the spatial length [7]. Note that an outlong cross-term vanishes in the expression for G for our $|\eta| < 0.35$ acceptance at midrapidity [18]. The fitted λ is empirically defined and includes contributions from misidentified particles $(1-f)^2$ along with components of the source that are not well resolved by the Gaussian fit.

Figure 1 shows the 3D correlation function of charged kaons without the Coulomb correction measured for $0.3 < k_T < 1.5$ GeV/c at 0%–30% centrality in Au + Au collisions at $\sqrt{s_{\rm NN}} = 200$ GeV and the fit with Eq. (1). Separate fits to the $2K^+$ and $2K^-$ correlation functions were performed, yielding consistent results for all k_T and centrality bins.

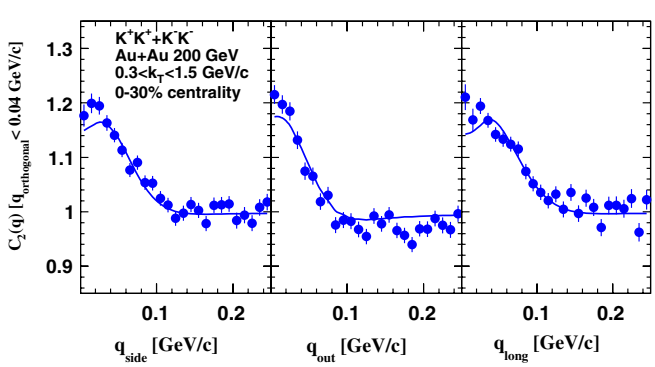

FIG. 1 (color online). 3D correlation function of charged kaon pairs. The curve is a 3D fit of Eq. (1) to the Coulomb uncorrected correlation, sliced over the lowest 40 MeV/c in the orthogonal directions.

Panels (a)–(e) in Fig. 2 show the HBT radius parameters of charged kaons for $0.3 < k_T < 1.5$ GeV/c as functions of $N_{\rm part}^{1/3}$, which is proportional to the transverse radius of the initial collision volume. Similar to pions, kaon radii are well described by linear functions of $N_{\rm part}^{1/3}$. Because initial fits yielded slopes that were consistent for all radii and intercepts that were consistent with zero, all three radii were fit to a single linear function with zero intercept: $R_{\rm ALL} = p_1 N_{\rm part}^{1/3}$, with $p_1 = 0.51 \pm 0.01$ and $\chi^2/{\rm ndf} = 14.6/8$. Although pions and kaons are measured in a

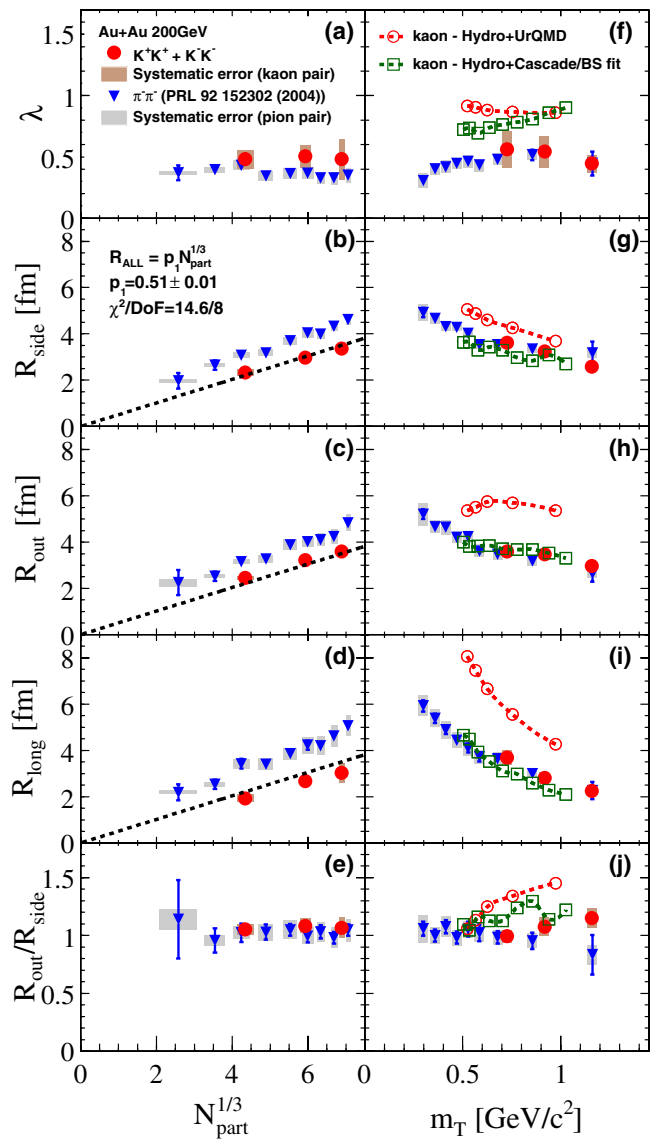

FIG. 2 (color online). 3D Gaussian HBT radius parameters extracted from Eq. (1) for charged kaon pairs as a function of (left) $N_{\rm part}^{1/3}$ measured for $0.3 < k_T < 1.5$ GeV/c and (right) m_T measured for 0%–30% centrality. In panels (b)–(d) the dashed line is a fit with $p_1 N_{\rm part}^{1/3}$. In panels (f)–(j) results from hydrodynamics models [22,23] are overlaid.

similar k_T range ($0.2 < k_T < 2.0$ GeV/c for pions), the higher transverse mass ($m_T = \sqrt{k_T^2 + m^2}$) for kaons ($\langle m_T \rangle \sim 0.89$ GeV/c^2) than for pions ($\langle m_T \rangle \sim 0.47$ GeV/c^2) leads to smaller radii, as expected from $\langle m_T \rangle$ scaling [17,19–21].

Panels (f)–(j) in Fig. 2 show the m_T dependence of the radius parameters for kaons in 3 different m_T bins at 0%–30% centrality, compared with pions [11]. HBT radii are quite consistent at the same m_T, clearly indicating that the radii follow m_T scaling. The $R_{\rm out}/R_{\rm side}$ ratio for kaons is ~1.0–1.2 which is consistent with the value for pions at low m_T. Kaon HBT results from a 2D + 1 hybrid, hydrodynamic + UrQMD calculation (open circles) [22] show slightly larger sidewards radii than the data, and the outwards and longitudinal components are too large by a factor of 2–3. A more recent 1D + 1 hybrid calculation [23] for kaons (open squares), which assumes flat rapidity distribution and axial symmetry, compares more favorably, matching all radii to within systematic and statical errors. This calculation incorporates preequilibrium flow and a lattice-inspired equation of state, which are two features lacking in earlier calculations of HBT radii. Although promising, these theoretical results remain to be verified with full 3D + 1 calculations that can also reproduce the elliptic flow.

We obtain a 1D HBT radius parameter of $R = 3.59 \pm 0.07(\text{stat}) \pm 0.18(\text{syst})$ fm for charged kaons with $\langle m_T \rangle = 1.03$ GeV/c^2, which is consistent with earlier STAR measurements for neutral kaons [10]. The resulting value for $\lambda = 0.42 \pm 0.03 \pm 0.08$ is lower than the neutral kaon value, but within 2 standard deviations.

Recent femtoscopic measurements [5,6], which use an imaging technique [24] revealed that the emission source function of charged pions has a non-Gaussian tail which cannot be resolved with traditional Gaussian fitting techniques. The correlation function is expressed by the Koonin-Pratt equation [25,26]

$$C_2(\mathbf{q}) - 1 = \int d\mathbf{r} K(\mathbf{q}, \mathbf{r}) S(\mathbf{r}), \tag{3}$$

where the kernel $K(\mathbf{q}, \mathbf{r})$ is the relative wave function as $|\Phi_{\mathbf{q}}^{(-)}(\mathbf{r})|^2 - 1$ that describes the propagation of pairs emitted with relative separation $\mathbf{r}$ and relative momentum $\mathbf{q}$ in the pair center-of-mass system (PCMS). $S(\mathbf{r})$ is the emission source function of pairs.

The filled squares in Fig. 3(a) show the 1D kaon correlation as a function of the invariant relative momentum of the pair [$q_{\rm inv} = \sqrt{-(p_1 - p_2)^2}/2$]. The 1D source function $S(r)$ imaged from $C_2(q_{\rm inv})$ is shown by filled circles in Fig. 3(b).

In this analysis, input parameters that govern the imaging procedure [24] were selected to minimize the χ^2 between the data and the restored $C_2(q_{\rm inv})$($\chi^2/\text{ndf} \sim 1$), shown by open circles in Fig. 3(a). The solid curve shows

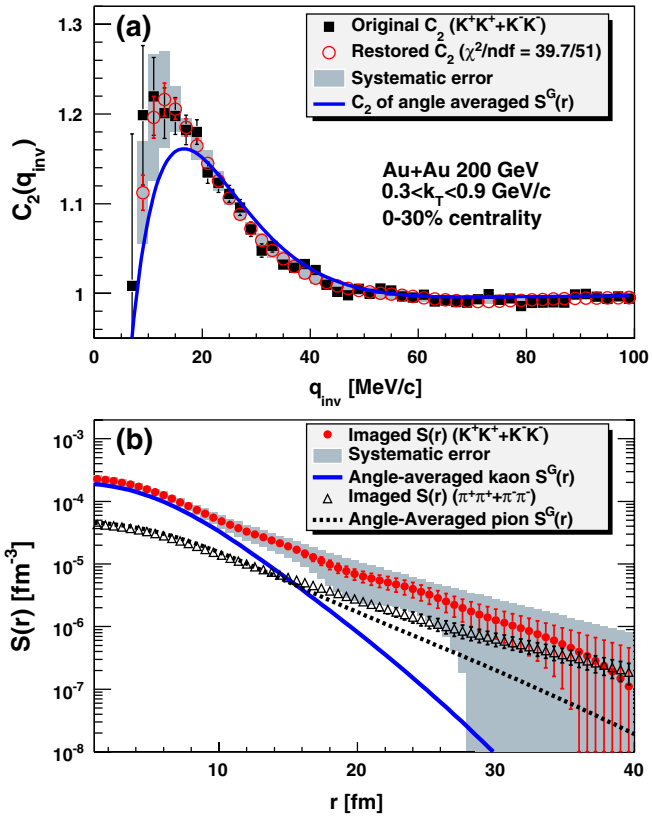

FIG. 3 (color online). (a) (filled squares) measured $C_2(q_{\rm inv})$. (open circles) restored $C_2(q_{\rm inv})$ from imaged $S(r)$, compared with (solid curve) angle-averaged Gaussian $C_2(q_{\rm inv})$ for charged kaon pairs. (b) (filled circle) Imaged kaon $S(r)$ compared with (solid curve) angle-averaged Gaussian $S(r)$. Error bars are statistical only and boxes indicate the total systematic errors. (open triangle) $S(r)$ for charged pion pairs for the same k_T region. For the pion $S(r)$, error bars include both statistical and systematic errors.

the traditional Gaussian source function, obtained by angle-averaging the 3D HBT radius parameters (λ, $R_{\rm side}$, $R_{\rm out}$, $R_{\rm long}$) in the PCMS frame, the same frame in which the imaging is performed.

The imaged $S(r)$ exhibits a non-Gaussian tail at $r \gtrsim 10$ fm. This excess corresponds to the deficit in the $q_{\rm inv} \lesssim 20$ MeV/c region of the angle-averaged Gaussian curve of Fig. 3(a), and is also visible in the 3D Gaussian slices in Fig. 1. The $S(r)$ for pions in the same k_T range shows a similar trend. The systematic error on the tail due to the kaon identification cut is ~3%. The deviation from a Gaussian in the shape of the $S(r)$ indicates that the particle emission region is extended, and a similar non-Gaussian tail in the pion source is not solely the result of long-lived resonance decays such as the ω, although a less prominent contribution from the K^* is likely. The observation of a more substantial non-Gaussian tail for kaons than for pions is qualitatively consistent with a hadronic resonance cascade model with a time dependent density for an expanding

source, in which the larger mean free path for kaons leads to an extended emission region [27,28]. Detailed measurements with 3D HBT imaging of kaons, or 1D imaging of more species probing different hadronic cross sections will determine contributions from other kinetic effects to $S(r)$.

In summary, we have measured Bose-Einstein correlation functions of charged kaon pairs in Au + Au collisions at $\sqrt{s_{\mathrm{NN}}} = 200$ GeV. The 3D HBT radii R_{side}, R_{out}, and R_{long} are consistent for pions and kaons at the same N_{part} and m_T. The 1D emission source function for kaons extracted by imaging shows a non-Gaussian tail at distances greater than 10 fm. This tail represents a direct measurement of the 1D length of homogeneity of the particle emission source and is not due primarily to resonance decays.

We thank the staff of the Collider-Accelerator and Physics Departments at BNL for their vital contributions. We acknowledge support from the Office of Nuclear Physics in DOE Office of Science and NSF (USA), MEXT and JSPS (Japan), CNPq and FAPESP (Brazil), NSFC (China), IN2P3/CNRS, and CEA (France), BMBF, DAAD, and AvH (Germany), OTKA (Hungary), DAE (India), ISF (Israel), KRF and KOSEF (Korea), MES, RAS, and FAAE (Russia), VR and KAW (Sweden), U.S. CRDF for the FSU, U.S.-Hungarian NSF-OTKA-MTA, and U.S.-Israel BSF.

*Deceased.
†PHENIX Spokesperson.
jacak@skipper.physics.sunysb.edu

[1] K. Adcox *et al.*, Nucl. Phys. **A757**, 184 (2005).
[2] T. Hirano and M. Gyulassy, Nucl. Phys. **A769**, 71 (2006).
[3] R. Hanbury Brown and R. Twiss, Philos. Mag. **45**, 663 (1954).
[4] G. Goldhaber, S. Goldhaber, W.-Y. Lee, and A. Pais, Phys. Rev. **120**, 300 (1960).
[5] S. S. Adler *et al.*, Phys. Rev. Lett. **98**, 132301 (2007).
[6] S. Afanasiev *et al.*, Phys. Rev. Lett. **100**, 232301 (2008).
[7] M. A. Lisa, S. Pratt, R. Soltz, and U. Wiedemann, Annu. Rev. Nucl. Part. Sci. **55**, 357 (2005).
[8] S. Soff, S. A. Bass, D. H. Hardtke, and S. Y. Panitkin, Phys. Rev. Lett. **88**, 072301 (2002).
[9] S. Bernard, D. H. Rischke, J. A. Maruhn, and W. Greiner, Nucl. Phys. **A625**, 473 (1997).
[10] B. I. Abelev *et al.*, Phys. Rev. C **74**, 054902 (2006).
[11] S. S. Adler *et al.*, Phys. Rev. Lett. **93**, 152302 (2004).
[12] K. Adcox *et al.*, Nucl. Instrum. Methods Phys. Res., Sect. A **499**, 469 (2003).
[13] R. J. Glauber and G. Matthiae, Nucl. Phys. **B21**, 135 (1970).
[14] S. Pratt, Phys. Rev. Lett. **53**, 1219 (1984).
[15] Y. Sinyukov, R. Lednicky, S. V. Akkelin, J. Pluta, and B. Erazmus, Phys. Lett. B **432**, 248 (1998).
[16] R. Maj and S. Mrowczynski, Int. J. Mod. Phys. E **16**, 3244 (2007).
[17] A. N. Makhlin and Y. M. Sinyukov, Z. Phys. C **39**, 69 (1988).
[18] S. Chapman, P. Scotto, and U. W. Heinz, Phys. Rev. Lett. **74**, 4400 (1995).
[19] I. G. Bearden *et al.*, Phys. Rev. Lett. **78**, 2080 (1997).
[20] M. Csanád and T. Csörgő, Acta Phys. Pol. Suppl. **1**, 521 (2008).
[21] T. Csörgő and B. Lörstad, Phys. Rev. C **54**, 1390 (1996).
[22] S. Soff arXiv:hep-ph/0202240.
[23] S. Pratt, Phys. Rev. Lett. **102**, 232301 (2009), and private communication for kaon data.
[24] D. A. Brown and P. Danielewicz, Phys. Lett. B **398**, 252 (1997).
[25] S. E. Koonin, Phys. Lett. B **70**, 43 (1977).
[26] S. Pratt, T. Csörgő, and J. Zimányi, Phys. Rev. C **42**, 2646 (1990).
[27] T. Csörgő, S. Hegyi, T. Novák, and W. A. Zajc, AIP Conf. Proc. **828**, 525 (2006).
[28] M. Csanád, T. Csörgő, and M. Nagy, Braz. J. Phys. **37**, 1002 (2007).